Metastable thermal donor states in germanium: Identification by electron paramagnetic resonance

H. H. P. Th. Bekman, T. Gregorkiewicz, I. F. A. Hidayat, and C. A. J. Ammerlaan
Natuurkundig Laboratorium, Universiteit van Amsterdam, Valckenierstraat 65, NL-1018 XE Amsterdam, The Netherlands

P. Clauws
Laboratorium voor Kristallografie en Studie van de Vaste Stof, Rijksuniversiteit Gent, Krijgslaan 281-S1, B-9000 Gent, Belgium
(Received 1 February 1990; revised manuscript received 16 August 1990)

One of the electron paramagnetic resonance (EPR) spectra related to thermal donors in germanium ("spectrum 1") has been studied in detail. The mutual identification of spectrum 1 and the F series of far-infrared (ir) donor energy levels has been established following observation of the effect of 100% bistability of that particular thermal-donor species. To our knowledge this is the first time that the bistability of the thermal-donor center has been observed in EPR. It has been further established that for the full description of spectrum 1 a higher spin value $S=1$ was necessary and the spin Hamiltonian had to be supplemented with an unusual higher-order term of the form B^2S^2.

I. INTRODUCTION

During the past three decades a tremendous amount of experimental data on silicon thermal donors (TD's) has been published. Far less is known about the germanium thermal donors. Donor activity of oxygen in germanium was first discovered by Elliot in 1957.[1] Intrinsic germanium crystals that were doped with oxygen in a zone-leveling apparatus turned to n-type conductivity, and it was possible to influence the electrical resistivity strongly by heat treatment of the crystal. Germanium thermal donors have striking similarities with silicon thermal donors; among others we mention the following: (1) Thermal donors in germanium and silicon can be generated only in oxygen-rich material by thermal anneals in the 300–550 °C region.[2,3] (2) The donor concentration reaches a maximum, after which it decreases to establish an equilibrium donor concentration.[4,5] (3) At higher annealing temperatures donor formation is faster, while the equilibrium concentration is lower.[6,7] (4) In infrared (ir) and photothermal ionization spectroscopy (PTIS) one can distinguish series of transitions that originate from several similar effective-mass (double) donors.[8–11] (5) The thermal donors are developing subsequently one species after the other, suggesting some kind of growth process.[12,13] (6) The early thermal donors are bistable. They are infrared active in the metastable state.[14–17]

An important difference between silicon and germanium thermal donors is the much larger concentration of the latter ones when generated under comparable conditions. For example at 450 °C, silicon containing 10^{18} cm^{-3} oxygen generates a maximum of about 2×10^{16} cm^{-3} donors compared to an estimated 2.5×10^{17} cm^{-3} donors for a similar germanium crystal. Most important, the rates of donor formation in germanium are at least 500 times greater than in silicon for similar temperature and oxygen concentrations. This can probably be explained by the difference in the oxygen diffusion coefficient in silicon and germanium. For silicon the diffusion coefficient is $D_{Si}[O_i]=0.07\exp(-2.44\ eV/kT)$ cm^2s^{-1} (Ref. 18), while for germanium it is below 500 °C more than 10^3 times higher: $D_{Ge}[O_i]=0.4\exp(-2.08\ eV/kT)$ cm^2s^{-1} (Ref. 19).

All the above-mentioned characteristic features argue for a similar defect model for thermal-donor centers in both materials. A theoretical study by LaPorta *et al.*[20] already showed that a similar defect model, and a similar defect formation process model, could explain the hierarchy of donor levels in silicon as well as in germanium. Therefore a study of thermal donors (TD's) in germanium could reveal important information that would then also be applicable to silicon TD's. At the same time such a study would have the advantage of being experimentally easier due to a higher concentration of centers and larger anisotropy of electron paramagnetic resonance (EPR) spectra.

Microscopic models for thermal donors in silicon relied at first for the most part on the conclusions obtained from electron paramagnetic resonance experiments. EPR measurements revealed two prominent centers labeled Si-NL8 and Si-NL10.[21,22] Both centers are strongly related to silicon thermal donors. Both centers show C_{2v} symmetry. Later detailed microscopic information was obtained from electron nuclear double resonance (ENDOR) studies of both centers.[23–26] The ENDOR results established for the first time that oxygen was actually involved in the defect structure of the thermal donor. Nevertheless no unanimously accepted defect model had been developed. New important structural information could be obtained if the mechanism behind the bistable behavior of the early thermal donors was understood. Therefore one can expect that this topic will attract much attention in future.

Recently Callens *et al.*[27] reported on the observation of new paramagnetic centers in oxygen-rich germanium with high thermal-donor contents. At least one of the spectra (labeled "spectrum 1") was related to thermal donors on basis of production characteristics as well as its g-factor values, which were characteristic for shallow effective-mass-like donors. The spectrum had C_{2v} sym-

metry and was in this way similar to the EPR spectra in silicon, while at the same time its anisotropy ($g_1=1.190$, $g_2=1.917$, $g_3=1.575$) was much bigger. The larger anisotropy can be explained by a stronger spin-orbit coupling coefficient of germanium and also by a higher ratio of longitudinal-to-transverse effective masses for the conduction-band minima.

It is the purpose of this research to investigate the bistable properties of the thermal-donor centers in germanium using the three recently discovered TD-related spectra. In the same kind of sample the bistable thermal donors were also investigated with use of far-ir spectroscopy, and consequently the correlation between the ir series and the EPR spectra was examined. In the case of silicon thermal donors, EPR spectra Si-NL8 and Si-NL10 are both superpositions of several spectra generated by individual thermal-donor species.[23-26] The different species are therefore not resolved in the EPR experiment, and consequently the bistable properties of the first two thermal-donor species are very difficult to detect. In germanium the anisotropy of the g tensor is more pronounced, offering, therefore, a possibility of assigning separate EPR spectra to individual thermal-donor species. This could then possibly be confirmed by comparing the bistable behavior of individual species as monitored in parallel by EPR and ir absorption.

II. EXPERIMENTAL

A. Equipment

The EPR measurements were performed with a superheterodyne spectrometer operating at 23 GHz and adjusted to detect the dispersion part of the signal. The magnetic field was modulated at a frequency of 83 Hz. A cylindrical TE_{011}-mode silver-coated Epibond cavity was used. The sample was held at a pumped helium temperature of about 1.6 K. The measurements were performed with the sample in the dark. During the cool down of the sample from room temperature we could illuminate the sample through a quartz rod in order to freeze the thermal donors in their metastable state. The light was produced by a halogen source.

The far-ir absorption measurements were done with a Fourier-transform spectrometer equipped with a helium-cooled germanium bolometer. Band-gap light was applied by a tungsten source and a monochromator set at 1.6 μm wavelength.

B. Samples

In the study two kinds of oxygen-rich, n-type germanium samples were used.

(1) Samples in the as-grown state: $[O_i]=2\times10^{17}$ cm^{-3}, and $[P]=10^{11}-10^{12}$ cm^{-3}. The number of carriers at various temperatures is 300 K—1.0×10^{16} cm^{-3}; and 77 K—3.9×10^{15} cm^{-3} (cooled in the dark) and 6.5×10^{15} cm^{-3} (cooled with light).

(2) Samples in the annealed state: $[O_i]=2\times10^{17}$ cm^{-3} and $[P]=10^{11}-10^{12}$ cm^{-3}. These samples received a thermal treatment of two stages: (a) dispersion: 5-min anneal at 900 °C followed by a room-temperature quench in the ambient and (b) thermal donor formation: 22 min at 350 °C. As a result the following number of carriers was developed as measured at various temperatures: 300 K—3.0×10^{15} cm^{-3}, and 77 K—1.3×10^{15} cm^{-3} (cooled in the dark) and 2.7×10^{15} cm^{-3} (cooled with light).

The samples had dimensions of $10\times1.5\times1.5$ mm^3, the longest dimension corresponding to $\langle 0\bar{1}1\rangle$, was along the axis of the microwave cavity. The magnetic field in the EPR measurement could therefore be rotated in the $(0\bar{1}1)$ plane.

III. EXPERIMENTAL RESULTS

A. Far-ir and electrical measurements

Samples for ir and conductivity measurements were cut adjacent to those selected for EPR.

The as-grown sample (type 1) had a TD concentration that was too high for a detailed absorption spectrum to be recordable. The high TD concentration results in high absorption, broad lines, and spectral congestion. The observation that the spectrum extended into the lower wave-number range indicated that shallower (i.e., later) TD members H, I, etc.[12] are likely to be present. The electrical measurements revealed that in this kind of sample about 40% of the TD's show bistable behavior; due to the reasons mentioned above, it was, however, impossible to establish which of the TD species were responsible for this effect.

The situation was more favorable for the annealed sample (type 2). Although the absorption was still too high and not detailed enough in the $2p_\pm, 3p_\pm$ range and above, a clear spectrum was obtained in the range of the $1s\rightarrow2p_0$ lines as given in Fig. 1; the $2p_0$ lines are sharper and weaker than the $2p_\pm$ lines, making them more appropriate for identification at TD concentrations of about 10^{15} cm^{-3}; positions of relevant lines of TD's in germanium are listed in Table I. After cooling under illumination, the TD species F, G, and H were detected—Fig. 1(a). When the sample was cooled in the dark, the lines of donor F had disappeared, while those of G and H remained unchanged—Fig. 1(b). This result demonstrates that the bistability of the annealed sample is entirely due to thermal donor F. Moreover, the amount of bistable TD's that can be estimated from the comparison of Figs. 1(a) and 1(b), agrees well with the 50% bistable donors revealed by the electrical measurements as shown in Sec. II B.

The present result is different from the previous observation by Clauws and Vennik,[15] who found that samples with lower initial oxygen concentration $[O_i]$ and low TD concentration of only 10^{14} cm^{-3} exhibited metastability of the earlier (i.e., deeper) D,E,F' species, while F,G,H remained stable shallow donors (see Table I for the identifications). This different behavior of species F in samples with low and high TD concentration seems to substantiate the remark made in Ref. 15 concerning the dependence of bistability on Fermi-level position, the

TABLE I. Identification of different TD series by their main far-ir absorption lines (Clauws and Vennik[12,15]). The 1*s* ground-state energy given in the last line is obtained by assuming the $3p_{\pm}$ level to coincide with the effective-mass theory value of 1.04 meV, except for donor *F* where the $2p_{\pm}$ value of 1.73 meV is used.

Transition level	Energy (cm^{-1} meV) for species					
	D	*E*	*F'*	*F*	*G*	*H*
$1s \rightarrow 2p_0$	99.2	96.5	92.7	93.1	90.2	87.2
				91.7	88.7	86.8
						(84.5)
$1s \rightarrow 2p_{\pm}$	132.0	128.0	125.1	125.7	123.9	120.9
	132.3		125.5			
1*s*	18.13	17.57	17.28	17.3	17.13	16.79

latter being itself a function of the donor concentration.

The configuration coordinate diagram of Fig. 2 explains bistable behavior of TD's in terms of capture against a barrier (see, e.g., Ref. 14). The presence of illumination during cooling transfers the deep configuration into the shallow one which then remains frozen at low temperature.

B. EPR measurements

As mentioned above, the bistable thermal donors can be frozen into their metastable, shallow donor state by cooling from room temperature under illumination with band-gap light. Such behavior of TD centers was also observed in our EPR experiment for both kinds of samples. If we cooled the annealed or as-grown sample slowly from room-temperature to pumped helium under illumination, we could confirm the EPR results of Callens *et al.*[27] The annealed sample mainly showed spectrum 1 and had traces of spectra 2 and 3 (see Table II for their approximate *g* values). In the as-grown sample spectrum 1 was very weak, while spectra 2 and 3 increased their intensities. If we cooled the samples (of both kinds) in the dark, the thermal donors remained in their stable state. The effect of the cooling procedure on the EPR spectra is depicted in Fig. 3. From the analysis of the EPR spectra one can deduce that the bistability is entirely due to spectrum 1. After cooling in the dark the intensity of spectrum 1 dropped below our detection limit. Spectra 2 and 3 did not change their intensity within the experimental error. Regardless of the cooling procedure no new spectra were observed.

In the paper by Callens *et al.*[27] the complete analysis of spectrum 1 was not possible as no appropriate spin Hamiltonian could be found. The "averaged" spectrum could be fitted with C_{2v} symmetry and $S = \frac{1}{2}$. The principal *g* values deduced in that way could be fully explained within the effective-mass theory. Figure 4(a) shows the angular dependence of spectrum 1 together with the averaged fit. As can be seen from the measurement, every

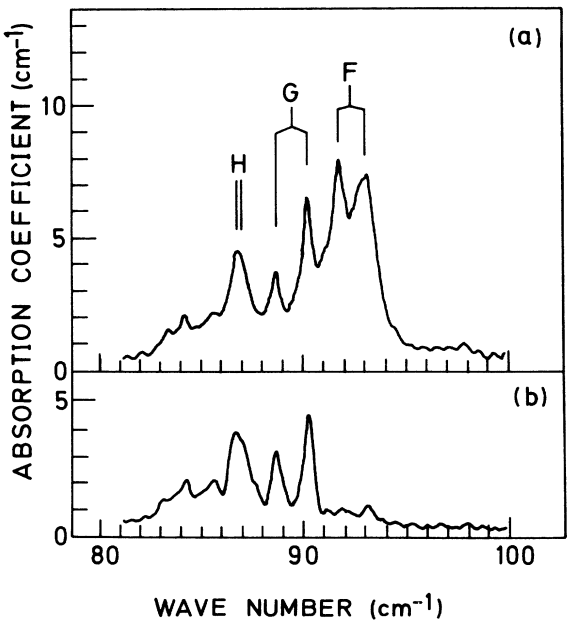

FIG. 1. Absorption spectrum of the annealed sample, $1s \rightarrow 2p_0$ lines: identification of thermal donors *F*, *G*, and *H* according to line positions given in Table I. (a) cooling under illumination and (b) cooling in the dark.

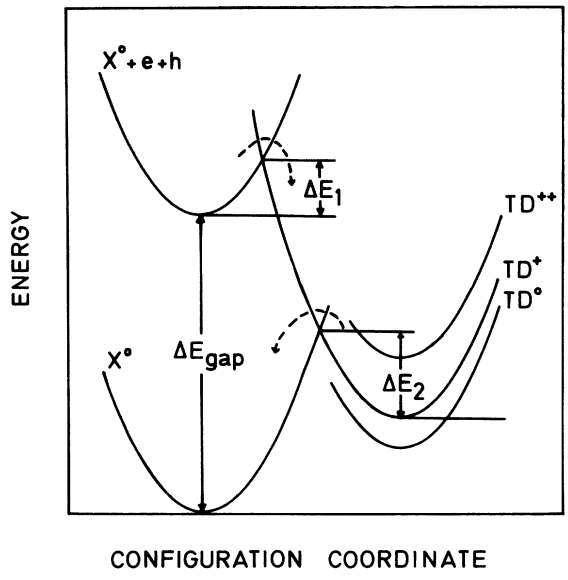

FIG. 2. Configuration coordinate diagram for bistable thermal donors (Refs. 14 and 16).

TABLE II. Principal g values of the three thermal donor spectra, as discovered by Callens *et al.* (Ref. 27). A question mark indicates that the value is not known.

	g_1	g_2	g_3
Spectrum 1	1.190 [110]	1.917 [$\bar{1}$10]	1.575 [001]
Spectrum 2	0.781 [111]	1.773 [11$\bar{2}$]	?
Spectrum 3	0.919 [111]	2.032 [11$\bar{2}$]	?

line of the C_{2v} pattern is split into two. The angular dependence excluded the possibility that the splitting was due to two similar $S=\frac{1}{2}$ centers. Attempts to fit the spectrum with $S=1$ and a spin Hamiltonian of the form

$$\mathcal{H}=\mu_B \mathbf{B}\cdot\vec{g}\mathbf{S}+\mathbf{S}\cdot\vec{D}\cdot\mathbf{S} \quad (1)$$

also failed. In particular it appeared to be impossible to reproduce a pattern of double crossing as indicated by the arrows in Fig. 4(a). We have made a detailed recording of the spectrum as depicted in Fig. 4(b) at K-band microwave frequency. In that way we could reveal the frequency dependence of these splittings. In Table III we have tabulated the splitting of the two lines, which show the peculiar double crossing, for X- and K-band microwave frequency. As can be noted, the ratio of the splitting in X and K bands is neither 1 nor equal to the frequency ratio (and is thus neither indicative for hyperfine nor for g-value splitting, respectively). Upon close inspection it appears to be equal to the square of the frequency ratio $(22.8/9.3)^2=6.01$. In what follows several spin Hamiltonians are considered in respect to whether the full description of experimental data could be provided and in particular as to whether the measured X- to K-band splitting ratio could be reproduced.

(1) A spin Hamiltonian for $S=\frac{1}{2}$ with only the electron-Zeeman term, with a g tensor with a symmetry lower than C_{2v}. This Hamiltonian does not produce the double crossing as indicated by arrows in Fig. 4(a). Furthermore, a splitting would be proportional to the ratio of K- and X-band microwave frequencies.

(2) A spin Hamiltonian for $S=\frac{1}{2}$ and $I=\frac{1}{2}$ containing electron-Zeeman, nuclear-Zeeman, and hyperfine interaction. This requires a 100% abundant nucleus with $I=\frac{1}{2}$.

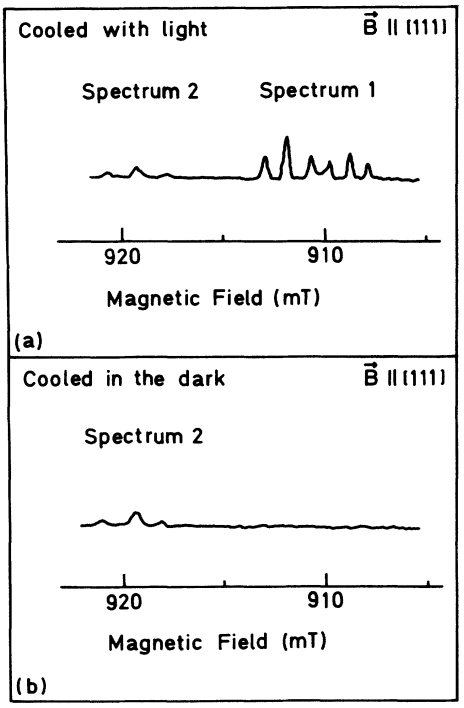

FIG. 3. Effect of cooling conditions on the EPR spectra as recorded at K-band microwave frequency at temperature 1.6 K. (a) Cooled with band-gap light and (b) cooled with sample in the dark.

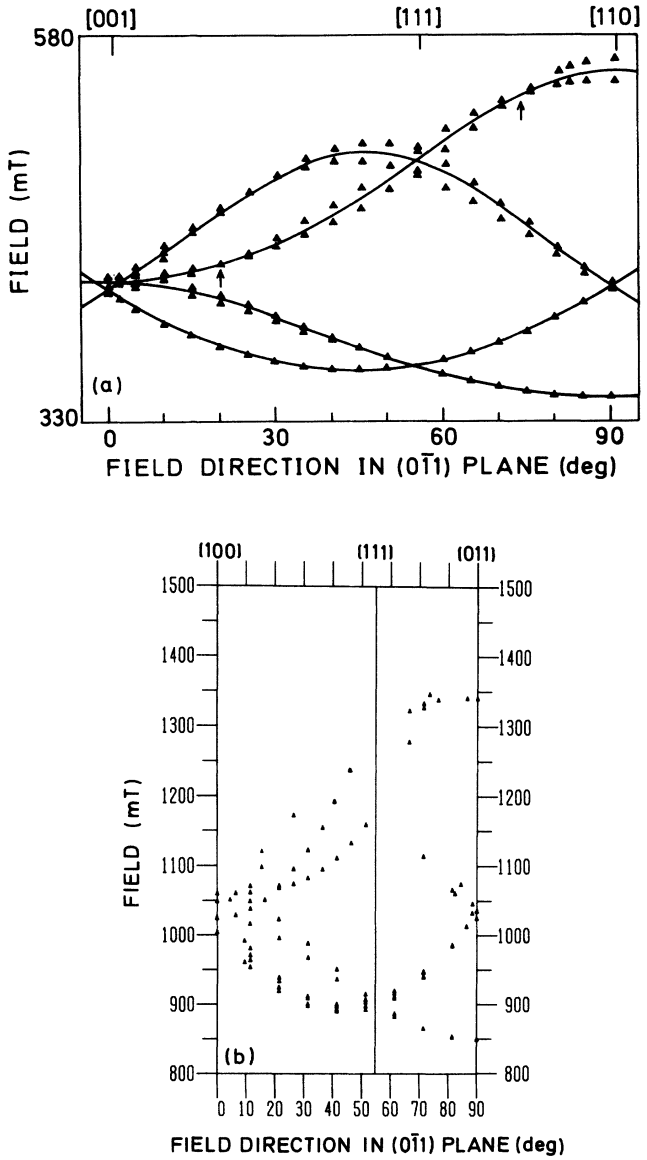

FIG. 4. (a) EPR data points of Callens *et al.* (Ref. 27), together with the averaged C_{2v} fit of spectrum 1. The measuring frequency was 9.3 GHz. (b) EPR data points as measured at the K band for spectrum 1. The sample was cooled under illumination. The measuring temperature was 1.6 K and the frequency was 22.800 181 GHz.

TABLE III. Magnetic-field splitting (in mT) of the two EPR lines that show a double crossing of spectrum 1.

Angle (deg)	K band	X band	Ratio	Angle (deg)	K band	X band	Ratio
0	−36.0	−6.0	6.0	50		14.6	
5	−34.0	−5.6	6.1	55		14.9	
10	−26.5	−4.3	6.2	60		13.2	
15	−15.5	−2.8	5.5	65	53.0	8.7	6.1
25	15.0	2.3	6.5	70	16.0	3.2	5.0
30	34.5	5.4	6.4	75	−23.5	−2.9	8.1
35	54.5	8.7	6.3	80		−9.2	
40	73.5	11.3	6.4	85		−13.4	
45	91.0	13.4	6.8	90		−14.7	

Possible candidates are hydrogen, fluor, and phosphorus. The possibility of interactions with any of these nuclei is rather unlikely except for phosphorus, although even in this case the available concentration is probably too low (10^{11}—10^{12} cm^{-3}). Also, however, this spin Hamiltonian cannot produce the double crossing. Moreover, if the splitting would be caused by the hyperfine interaction, then its magnitude should be the same for both microwave bands.

(3) A spin Hamiltonian for $S=1$ with the electron-Zeeman and zero-field splitting terms. This Hamiltonian also cannot produce the double crossing. The splitting between the two lines has to be produced by the zero-field splitting term. The D term splits the $1\leftrightarrow2$ and the $2\leftrightarrow3$ EPR transition; see Fig. 5. The splitting is again independent of microwave frequency. In order to have a splitting proportional to the square of the frequency ratio a quadratic dependence of D parameter on magnetic field, i.e., $D \propto B^2$ would be required.

Generally speaking, the effective spin Hamiltonian is composed of terms expressed as $S^a I^b B^c$, where S, I, and B are the electron spin, the nuclear spin and the external magnetic field, respectively. The sum $a+b+c$ must be an even integer due to the time-reversal symmetry. Therefore spin-Hamiltonian terms such as B^2S^2, B^3S, etc., i.e., with higher powers of B, are also allowed. However, the effects due to these terms are usually very small when compared to the bilinear or quadratic terms, as their coefficients come from higher-order mixing effects between the ground state and higher-energy states. To our knowledge there are only three cases reported in the literature where terms proportional to B^2 had to be included in the Hamiltonian. These are Cr^0 in Si,[28] Zr^{3+} in ZnSe, and Dy^{3+} in CaF_2.[29] For these centers, already in the microwave region, the nearby excited levels are not much higher than the Zeeman energy. Following the observed splitting ratio we have included a B^2S^2-term in our spin Hamiltonian. Here two possibilities could be taken into consideration:

$$\mathcal{H}=\mu_B \mathbf{B}\cdot\vec{\mathbf{g}}\cdot\mathbf{S}+\mathbf{S}\cdot\vec{\mathbf{D}}\cdot\mathbf{S}+\lambda B^2S^2 , \tag{2}$$

$$\mathcal{H}=\mu_B \mathbf{B}\cdot\vec{\mathbf{g}}\cdot\mathbf{S}+\lambda B^2S^2 , \tag{3}$$

where in C_{2v} symmetry λB^2S^2 is a short notation for

$$\begin{aligned}&S_x^2(\lambda_{xxxx}B_x^2+2\lambda_{xxxy}B_xB_y+\lambda_{xxyy}B_y^2+\lambda_{xxzz}B_z^2)+S_y^2(\lambda_{xxxx}B_y^2+2\lambda_{xxxy}B_xB_y+\lambda_{xxyy}B_x^2+\lambda_{xxzz}B_z^2)\\&+S_z^2(\lambda_{zzzz}B_z^2+\lambda_{xxzz}B_x^2+\lambda_{xxzz}B_y^2+2\lambda_{xyzz}B_xB_y)\\&+(S_xS_y+S_yS_x)(\lambda_{xxxy}B_x^2+\lambda_{xxxy}B_y^2+2\lambda_{xxyy}B_xB_y+\lambda_{xyzz}B_z^2)\\&+(S_xS_z+S_zS_x)(2\lambda_{xxzz}B_xB_z+2\lambda_{xyzz}B_yB_z)+(S_yS_z+S_zS_y)(2\lambda_{xxzz}B_yB_z+2\lambda_{xyzz}B_xB_z) .\end{aligned} \tag{4}$$

The spin Hamiltonian of Eq. (2) gives a slightly better fit than the Hamiltonian of Eq. (3). Both spin Hamiltonians produce the double crossing behavior. However, the constant ratio of the splitting at K- and X-band microwave frequency as tabulated in Table III is only reproduced by the spin Hamiltonian of Eq. (3). The result of the fit is depicted in Fig. 6(a). A splitting due to misorientation is visible. The spin-Hamiltonian parameters as found from the fit are tabulated in Table IV. The g tensor is very close to the g tensor found in the averaged fit of Callens *et al.*;[27] see Table II. We have also made a simulation with this spin Hamiltonian for X band under assumption of no misorientation and an exactly 9.3-GHz microwave frequency value. As can be seen in Fig. 6(b), it is in good agreement with the experimental points as measured by

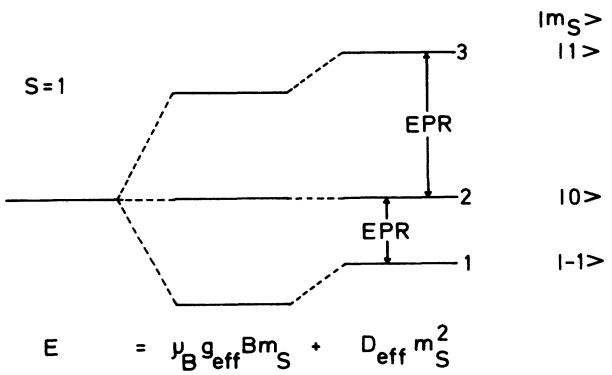

FIG. 5. Schematic energy-level diagram for an $S=1$ system. The allowed EPR transitions are indicated.

Callens *et al.*[27] In Fig. 7 we have depicted the splitting of the two lines with the double crossing as measured in the K and X bands, together with the fit for the K band and the simulation for the X band. As can be concluded from Figs. 6 and 7, the spin Hamiltonian of Eq. (3) provides a satisfactory description of the experimental data.

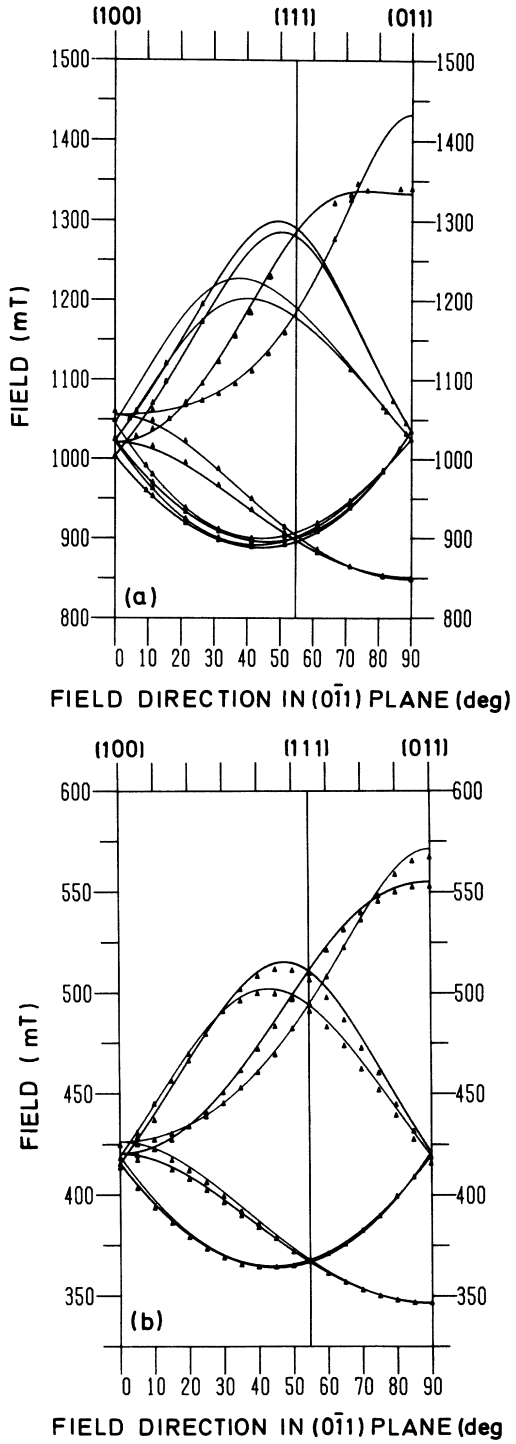

FIG. 6. (a) Result of the fit of spectrum 1 together with the fitted data points. (b) Simulation of spectrum 1 at 9.3 GHz with the parameters listed in Table IV. The data points of Callens *et al.* (Ref. 27) are also shown.

TABLE IV. Parameters obtained for the fit of spectrum 1 with the spin Hamiltonian of Eq. (3).

Parameter	Value	Units
g_1	1.1803	
g_2	1.9171	
g_3	1.5698	
λ_{xxxx}	−0.204	GHz/T^2
λ_{zzzz}	−0.188	GHz/T^2
λ_{xxxy}	0.062	GHz/T^2
λ_{xxyy}	−0.031	GHz/T^2
λ_{xxzz}	0.173	GHz/T^2
λ_{xyzz}	−0.219	GHz/T^2

IV. DISCUSSION

A. Correlation of EPR spectra and far-ir series

As described in the preceding paragraph, current EPR studies were performed in detail only for the annealed sample. They have revealed the dominant presence of spectrum 1, while spectra 2 and 3 were present in lower concentration. Out of these three, only spectrum 1 showed bistable behavior. At the same time, far-ir spectra on an adjacent sample detected the presence of thermal-donor series F, G, and H out of which only the F series showed bistability. Therefore it seems reasonable to identify the EPR spectrum 1 with the thermal-donor F series. In this way the present study supports the conclusion by Callens *et al.*[27] that spectrum 1 is thermal

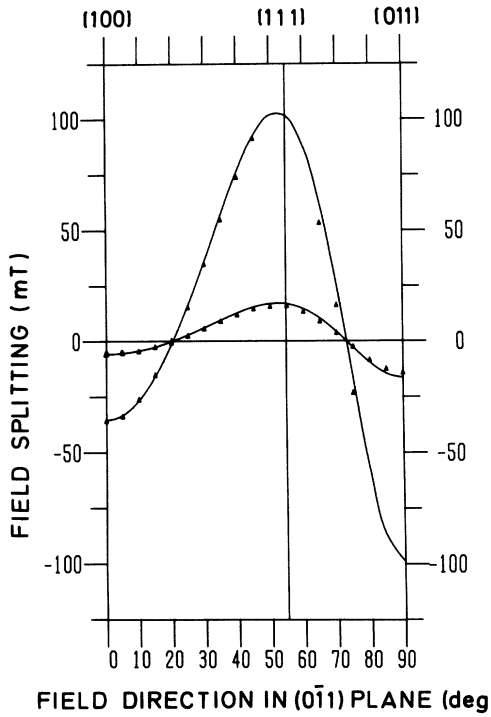

FIG. 7. Splitting of the two lines with the double crossing as fitted in K band and simulated in X band together with the experimental points.

donor related. Spectrum 1 is thus the EPR signature of an early thermal donor in the metastable state. In contrast with the situation in silicon, a single EPR spectrum, in this case spectrum 1, corresponds therefore to only one TD species. Although it is tempting to relate spectra 2 and 3 to far-ir series G and H, there appears so far to be insufficient evidence to support such identification. If spectra 2 and 3 are not related to G and H, then one should conclude that the G and H donors are not EPR active in their neutral charge state. It was further concluded by Callens *et al.* that spectra 2 and 3 were most probably of trigonal symmetry. If one identifies spectra 2 and 3 with the G and H series, then this would require a drastic structural change to occur in the growth process between thermal-donor species F and G, resulting in a symmetry change from C_{2v} to trigonal.

B. Triplet spin system

The samples used in this experiment have an n-type shallow impurity background (phosphorus). At the measuring temperature of 1.6 K the thermal donors that have shallow double-donor character are therefore in the neutral charge state, as is already the case at 7 K as shown by the ir absorption spectrum. In a covalent material such as germanium, two spins of electrons in bonds will pair off, resulting in an $S=0$ system for the ground state. Such a system is inaccessible by EPR measurements. Nevertheless the possibility of $S=1$ triplet ground state with a parallel spin arrangement cannot be *a priori* excluded for an impurity. A spin-triplet state $S=1$ would be paramagnetic and therefore observable by EPR. Spin-singlet and -triplet states have indeed been observed in silicon for other double donors such as S, Se, and Te.[30–32] For TD's in germanium, in the interpretation of their recent far-ir measurements, Clauws and Vennik[15] considered the existence of spin-singlet as well as spin-triplet states. Our present data on spectrum 1 support a description with $S=1$. A peculiarity in the fit to the experimental data is the B^2S^2 term appearing in the spin Hamiltonian. The spin-Hamiltonian terms nonlinear in the magnetic field occur only seldomly. They indicate that the nearby excited levels are not much higher in energy than the Zeeman energy and can therefore be mixed in, even in the microwave region. It is possible that the excited states are also paramagnetic and that one can observe resonance signals also from these states. However, no such EPR signals were detected.

C. Relation with silicon thermal donors

The only EPR spectrum observed in thermal-donor-rich n-type silicon is Si-NL10. In spite of extensive studies, the origin of this spectrum is still mysterious,[33] while at the same time its direct relation to silicon TD's is unambiguous. Because of all the similarities between germanium and silicon thermal donors, one is tempted to make a link between spectrum 1 in germanium and NL10 in silicon. Following that analogy Si-NL10 would then be identified with the triplet state $S=1$ of the normal silicon TD's. However, an ultimate test for the spin assignment for Si-NL10 ($S=\frac{1}{2}$ or 1) is provided by the electron nuclear double resonance (ENDOR) experiment. The ENDOR data obtained for NL10 were analyzed with the spin Hamiltonian:

$$\mathcal{H}=\mu_B \mathbf{B}\cdot\vec{\vec{g}}\cdot\mathbf{S}-\mu_N g_N \mathbf{B}\cdot\mathbf{I}+\mathbf{S}\cdot\vec{\vec{A}}\cdot\mathbf{I}+\mathbf{I}\cdot\vec{\vec{Q}}\cdot\mathbf{I}\ . \tag{5}$$

If we neglect the last term for simplicity, then the ENDOR transitions are given in first order by

$$h\nu=|\mu_N g_N B + A_{\text{eff}} m_S|\ . \tag{6}$$

In case of an $S=\frac{1}{2}$ system one expects two lines at $\mu_N g_N B \pm \frac{1}{2} A_{\text{eff}}$; for an $S=1$ system one has, however, three lines at $\mu_N g_N B \pm A_{\text{eff}}$ and $\mu_N g_N B$. On basis of the ENDOR data[26] an $S=1$ system can practically be excluded for the Si-NL10 spectrum.

V. CONCLUSIONS

We have identified the EPR spectrum 1 of thermal donors in germanium with the F series as revealed by the far-ir absorption measurements. The bistable behavior could be established for that center; spectrum 1 could only be observed if the sample was cooled under illumination. The spectrum could be described with $S=1$ spin value indicating triplet ground state. In order to fully account for the experimental data, the spin Hamiltonian had to be augmented by a higher-order term, namely, B^2S^2. The results of the present study indicate that, in contrast to the situation in silicon, different species of germanium TD's can be resolved in EPR.

ACKNOWLEDGMENTS

The authors gratefully acknowledge Metallurgie Hoboken-Overpelt for growing the oxygen-doped germanium and the Stichting voor Fundamenteel Onderzoek der Materie (FOM) for financial support.

[1]G. Elliot, Nature (London) **180**, 1350 (1957).
[2]J. Bloem, C. Haas, and P. Penning, J. Phys. Chem. Solids **12**, 22 (1959).
[3]C. S. Fuller, J. A. Ditzenberger, N. B. Hannay, and E. Buehler, Phys. Rev. **96**, 833 (1954).
[4]C. S. Fuller, J. Phys. Chem. Solids **19**, 18 (1961).
[5]C. S. Fuller and R. A. Logan, J. Appl. Phys. **28**, 1427 (1957).
[6]C. S. Fuller, W. Kaiser, and C. D. Thurmond, J. Phys. Chem. Solids **17**, 301 (1961).
[7]W. Kaiser, H. L. Frisch, and H. Reiss, Phys. Rev. **112**, 1546 (1958).
[8]P. Clauws, J. Broeckx, E. Simoen, and J. Vennik, Solid State Commun. **44**, 1011 (1982).
[9]B. Pajot, H. Compain, J. Lerouille, and B. Clerjaud, Physica B+C **117&118B**, 110 (1983).
[10]P. Clauws and J. Vennik, Phys. Rev. B **30**, 4837 (1984).

[11]D. Wruck and P. Gaworzewski, Phys. Status Solidi A **56**, 557 (1979).
[12]P. Clauws and J. Vennik, Mater. Sci. Forum **10-12**, 941 (1986).
[13]P. Wagner, in *Oxygen, Carbon, Hydrogen and Nitrogen in Crystalline Silicon,* edited by J. C. Mikkelsen, Jr., S. J. Pearton, J. W. Corbett, and S. J. Pennycook (Materials Research Society, Pittsburgh, 1986), p. 125.
[14]V. V. Litvinov, G. V. Pal'chik, and V. I. Urenev, Fiz. Tekh. Poluprovodn. **19**, 1366 (1985) [Sov. Phys. Semicond. **19**, 841 (1985)].
[15]P. Clauws and J. Vennik, Mater. Sci. Forum **38-41**, 473 (1989).
[16]L. F. Makarenko, V. P. Markevich, and L. I. Murin, Fiz. Tekh. Poluprovodn. **19**, 1935 (1985) [Sov. Phys. Semicond. **19**, 1192 (1985)].
[17]P. Wagner and J. Hage, Appl. Phys. A **49**, 123 (1989).
[18]U. Gösele, K.-Y. Ahn, B. P. R. Marioton, T. Y. Tan, and S.-T. Lee, Appl. Phys. A **48**, 219 (1989).
[19]J. W. Corbett, R. S. McDonald, and G. D. Watkins, J. Phys. Chem. Solids *25*, 873 (1964).
[20]C. S. LaPorta, J. C. Kimball, J. T. Borenstein, and J. W. Corbett, J. Phys. C **19**, L627 (1986).
[21]S. H. Muller, M. Sprenger, E. G. Sieverts, and C. A. J. Ammerlaan, Solid State Commun. **25**, 987 (1978).
[22]S. H. Muller, E. G. Sieverts, and C. A. J. Ammerlaan, in *Proceedings of the International Conference on Radiation Effects in Semiconductors, Nice, 1978,* Institute of Physics Conf. Ser. No. 46, edited by J. H. Albany (IOP, London, 1979), p. 297.
[23]J. Michel, J. R. Niklas, J.-M. Spaeth, and C. Weinert, Phys. Rev. Lett. **57**, 611 (1986).
[24]J. Michel, J. R. Niklas, and J.-M. Spaeth, in *Defects in Electronic Materials,* edited by M. Stavola, S. J. Pearton, and G. Davies (Materials Research Society, Pittsburgh, 1988), p. 185.
[25]H. H. P. Th. Bekman, T. Gregorkiewicz, and C. A. J. Ammerlaan, Phys. Rev. B **39**, 1648 (1989).
[26]T. Gregorkiewicz, H. H. P. Th. Bekman, and C. A. J. Ammerlaan, Phys. Rev. B **38**, 3998 (1988).
[27]F. Callens, P. Clauws, P. Matthys, E. Boesman, and J. Vennik, Phys. Rev. B **39**, 11 175 (1989).
[28]G. W. Ludwig and H. H. Woodbury, Solid State Phys. **13**, 223 (1962).
[29]E. S. Sabisky, J. Chem. Phys. **41**, 892 (1964).
[30]K. Bergman, G. Grossmann, H. G. Grimmeiss, and M. Stavola, Phys. Rev. Lett. **56**, 2827 (1986).
[31]K. Bergman, G. Grossmann, H. G. Grimmeiss, M. Stavola, C. Holm, and P. Wagner, Phys. Rev. B **37**, 10 738 (1988).
[32]R. E. Peale, K. Muro, A. J. Sievers, and F. S. Ham, Phys. Rev. B **37**, 10 829 (1988).
[33]T. Gregorkiewicz, H. H. P. Th. Bekman, and C. A. J. Ammerlaan, Phys. Rev. B **41**, 12 628 (1990).